

Development of a krypton-doped gas symmetry capsule platform for x-ray spectroscopy of implosion cores on the NIF

T. Ma, H. Chen, P. K. Patel, M. B. Schneider, M. A. Barrios, D. T. Casey, H.-K. Chung, B. A. Hammel, L. F. Berzak Hopkins, L. C. Jarrott, S. F. Khan, B. Lahmann, R. Nora, M. J. Rosenberg, A. Pak, S. P. Regan, H. A. Scott, H. Sio, B. K. Spears, and C. R. Weber

Citation: *Rev. Sci. Instrum.* **87**, 11E327 (2016); doi: 10.1063/1.4960753

View online: <http://dx.doi.org/10.1063/1.4960753>

View Table of Contents: <http://aip.scitation.org/toc/rsi/87/11>

Published by the [American Institute of Physics](#)



SHIMADZU
Excellence in Science

**Powerful, Multi-functional UV-Vis-NIR and
FTIR Spectrophotometers**

Providing the utmost in sensitivity, accuracy and resolution for applications in materials characterization and science

- Photovoltaics
- Polymers
- Coatings
- Paints
- Ceramics
- Thin films
- Inks
- DNA film structures
- Packaging materials
- Nanotechnology

[Click here for accurate, cost-effective laboratory solutions](#)



Development of a krypton-doped gas symmetry capsule platform for x-ray spectroscopy of implosion cores on the NIF

T. Ma,^{1,a)} H. Chen,¹ P. K. Patel,¹ M. B. Schneider,¹ M. A. Barrios,¹ D. T. Casey,¹ H.-K. Chung,² B. A. Hammel,¹ L. F. Berzak Hopkins,¹ L. C. Jarrott,¹ S. F. Khan,¹ B. Lahmann,³ R. Nora,¹ M. J. Rosenberg,⁴ A. Pak,¹ S. P. Regan,⁴ H. A. Scott,¹ H. Sio,³ B. K. Spears,¹ and C. R. Weber¹

¹Lawrence Livermore National Laboratory, Livermore, California 94550, USA

²International Atomic Energy Agency, Vienna, Austria

³Plasma Fusion and Science Center, Massachusetts Institute of Technology, Cambridge, Massachusetts 02139, USA

⁴Laboratory for Laser Energetics, University of Rochester, Rochester, New York 14623, USA

(Presented 8 June 2016; received 8 June 2016; accepted 20 July 2016; published online 18 August 2016)

The electron temperature at stagnation of an ICF implosion can be measured from the emission spectrum of high-energy x-rays that pass through the cold material surrounding the hot stagnating core. Here we describe a platform developed on the National Ignition Facility where trace levels of a mid-Z dopant (krypton) are added to the fuel gas of a symcap (symmetry surrogate) implosion to allow for the use of x-ray spectroscopy of the krypton line emission. *Published by AIP Publishing.* [<http://dx.doi.org/10.1063/1.4960753>]

I. INTRODUCTION

Accurately characterizing the stagnation conditions achieved in indirect drive inertial confinement fusion implosions¹ is key to achieving ignition on the National Ignition Facility (NIF).^{2,3} The inference of ion temperature from neutron spectral measurements in indirect-drive ICF implosions is known to be sensitive to non-thermal velocity distributions in the fuel.⁴ The measurement of electron temperature (T_e) inferred from x-ray emission should not be sensitive to these bulk motions and hence may be a better measure of the thermal temperature of the hot-spot.

A series of experiments have been conducted on the NIF where a small concentration of mid-Z dopant (krypton) is added to the fuel gas of a symcap⁵ implosion. The x-ray spectra are measured using a number of time-resolved and time-integrated, spectrally resolved x-ray diagnostics to evaluate the feasibility of using dopant line ratios for a T_e measurement.^{6–9} In ignition-relevant capsules, which cannot have a dopant in the fuel, electron temperature will be measured by the slope of the continuum x-ray emission, and this measurement can be benchmarked against the Kr-doped surrogate.

II. THE KRYPTON SYMCAP PLATFORM

A. Selection of a dopant

The addition of a dopant to a capsule fuel gas must be carefully chosen to satisfy competing constraints. To make a

direct measurement of the temperature of the hot core, the dopant must be added uniformly to the fuel constituting the hot-spot. In the case of a symcap implosion, which is filled with a gas, this means a dopant in gaseous form must be used. The dopant should preferably be non-toxic (for ease of fielding) and single species (for more straightforward interpretation of spectra). The dopant element must further have line emission that can escape the high areal density shell with minimal attenuation. Krypton ($Z = 36$), an inert noble gas, with K-shell lines >13 keV (see Fig. 1) fulfills these requirements.

In selecting a dopant fraction, the quantity of this dopant pre-mixed into the fuel gas must be high enough that enough characteristic line emission x-ray photons are produced to be detected by the diagnostics, but not so high as to significantly perturb the hot-spot dynamics (due to radiative cooling^{10,11} or kinetic effects¹²). Further, there must be minimal self-opacity of the lines of interest.

The multi-dimensional non-local thermodynamic equilibrium (NLTE) atomic kinetics/radiation transfer code Cretin¹³ was used to estimate the expected signal variation with dopant level for representative symcap implosions modeled with HYDRA.¹⁴ Based on this work, it was found that 0.01–0.03 at. % Kr dopant in the fill gas of a symcap was an adequate starting place, with the Kr He- β line becoming optically thick above those levels.

Besides the ability to escape the compressed shell, in order to be diagnostically useful, the chosen Kr lines should have an intensity ratio adequately sensitive over the range of expected implosion temperatures. From population kinetics FLYCHK¹⁵ simulations, the Kr He-like (He- β and dielectronic satellites on the lower energy side of the He- β) to Li-like ratio is found to increase $5\times$ over a T_e change from 2 to 4 keV, with only marginal sensitivity to electron density over the range of 5×10^{23} – 5×10^{24} (typical of the hot-spot electron density at

Note: Contributed paper, published as part of the Proceedings of the 21st Topical Conference on High-Temperature Plasma Diagnostics, Madison, Wisconsin, USA, June 2016.

^{a)}Author to whom correspondence should be addressed. Electronic mail: ma8@llnl.gov

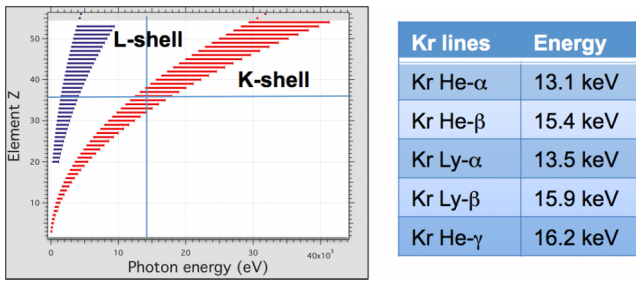


FIG. 1. The photon energy of L-shell and K-shell line emissions for various elements from $Z=3$ (Li) to $Z=54$ (Xe). The Kr K-shell lines (He-like and H-like) occur at energies >13 keV, and thus can escape the compressed dense shell of an ICF implosion.

stagnation), so can serve as a good diagnostic. See Fig. 2 for ratio sensitivity.

B. Experimental setup

The considerations for the platform design included choosing a low mix, round implosion in order to reduce x-ray emission due to higher-Z contamination (from hydrodynamic mix of the ablator)¹⁶ into the hot-spot. A high hot-spot temperature, and low ablator areal density (ρR) to minimize ablator opacity were also desired. An existing HDC (high density carbon) subscale symcap platform^{17,18} was chosen, using an undoped HDC shell of $64\ \mu\text{m}$ thickness, $908\ \mu\text{m}$ outer radius, in an Au hohlraum of 5.75 mm diameter, 10.1 mm length (Fig. 3). The implosion was driven with a 900 kJ, 300 TW laser pulse with 3 shocks. The hohlraum fill gas was “near-vacuum” of 0.03 mg/cc ^4He , and the capsule fill was 4.5 mg/cc DD (D_2 , Deuterium) with the trace levels of Kr. The 4.5 mg/cc fill is lower than the nominal symcap fill density of 8.5 mg/cc to allow the implosion to converge more and achieve higher hot-spot temperatures. Stagnation of the Au plasma bubble from ablation of the inside wall of the hohlraum was not found to be an issue in the platform, avoiding issues of the Au potentially blocking x-ray emission from the capsule.

The fielding temperatures for the experiment must be chosen to ensure the Kr does not condense out of the gaseous

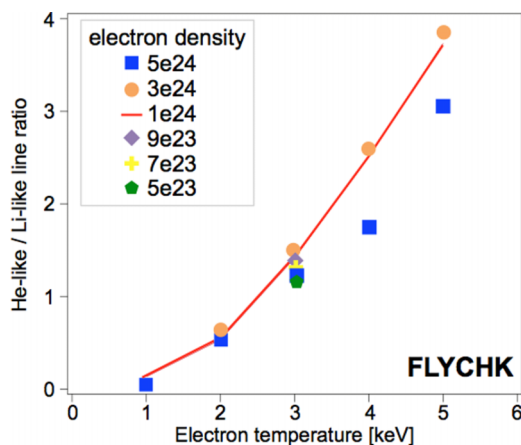


FIG. 2. The sensitivity in krypton He-like to Li-like line intensities as a function of electron temperature for varying electron densities.

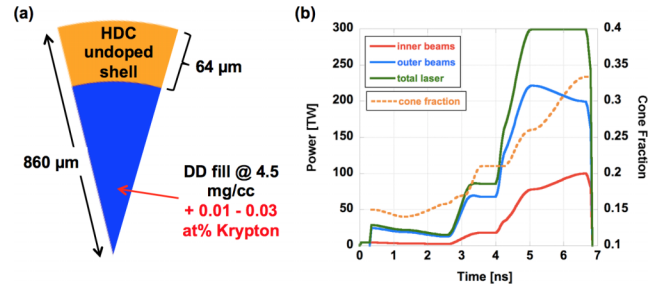


FIG. 3. (a) Pie diagram of the capsule. The capsule is filled with DD gas and 0.01 - 0.03 at. % Kr at 4.5 mg/cc. (b) The laser pulse shape and cone fraction (defined as inner laser cone power/total) for the drive used in these experiments.

state while in the capsule. Thus, in the series of experiments described here, as the Kr dopant fraction is varied at 0.01 at. %, 0.02 at. %, and 0.03 at. %, the fielding temperatures are set to 78 K, 80 K, and 82 K, respectively. The gas mixture of the delivered gas bottle was characterized by mass spectrometry prior to installation on the target fielding gas manifold and filling of the capsule. The mass spectrometry composition of Kr is calculated from the Kr-84 peak and a 2% Kr calibration sample. The actual Kr gas mixtures delivered for the experiments were 0.009 ± 0.0005 at. %, 0.022 ± 0.001 at. %, and 0.027 ± 0.003 at. %. The absolute error on the level of Kr reported is $\pm 10\%$.

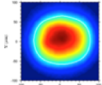
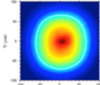
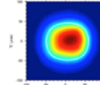
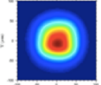
The x-ray emission was recorded with the NIF X-ray spectrometer (NXS).¹⁹ The NXS consists of a singly curved elliptical Bragg crystal, and for this set of experiments covered a spectral range of 10.8 – 18.2 keV at a resolving power $E/\Delta E$ of ≥ 60 . Three separate channels are simultaneously run on the NXS, allowing for different filtrations and the establishment of spectral dispersion by the use of the filter K-edges. For each of the three shots in this series, the NXS returned time-integrated spectra on imaging plate. Additionally, on the two higher dopant level shots, the NXS was also coupled to a DIM Insertable Streak Camera (DISC)^{20,21} to provide time-resolved spectra with ~ 100 ps temporal resolution in addition to the two time-integrated channels.

Further, standard x-ray imaging with pinholes onto the gated framing cameras provided time-resolved hot-spot shape and low-mode shape swings,^{22,23} while image plates recorded differentially filtered images for shape and a coarse T_e from x-ray emission.^{24,25} X-ray bang time and burnwidth was provided by the SPIDER (Streaked Polar Instrumentation for Diagnosing Energetic Radiation),²⁶ while the Wedge Range Filters (WRF)²⁷ gave an independent measure of total ρR along two lines of sight. A suite of neutron time-of-flight (NTOF) diagnostics^{28,29} provided nuclear metrics of DD yield and ion temperature (T_{ion}), and a particle-time-of-flight (PTOF)³⁰ gave a DD-compression bangtime.

III. RESULTS AND DISCUSSION

With increasing Kr dopant fraction, it was found that DD neutron yield, ion temperature, and x-ray burnwidth decreased, consistent with enhanced radiative cooling due to the increased fraction of high-Z dopant. The overall convergence of the

TABLE I. Comparison of performance metrics for the set of krypton shots.

	N140913-002 D ³ He @ 8.5 mg/cc	N150812-001 DD w/0.01 at. % Kr @ 4.5 mg/cc	N160228-002 DD w/0.02 at. % Kr @ 4.5 mg/cc	N160502-002 DD w/0.03 at. % Kr @ 4.5 mg/cc
DD yield	$2.7 \pm 0.2 \times 10^{11}$ (D ³ He)	$7.8 \pm 0.8 \times 10^{12}$ (DD w/Kr)	$2.3 \pm 0.1 \times 10^{12}$ (DD w/Kr)	$9.4 \pm 0.8 \times 10^{11}$ (DD w/Kr)
DD T ₁ (keV)	2.5 ± 0.3	2.8 ± 0.3	2.39 ± 0.3	2.02 ± 0.1
X-ray BT (ns)	8.15 ± 0.02	8.28 ± 0.03	8.27 ± 0.04	8.51 ± 0.06
X-ray burn (ps)	276 ± 17	296 ± 70	259 ± 30	255 ± 15
DD-n comp BT (ns)	8.27 ± 0.07	8.08 ± 0.05	8.15 ± 0.06	8.35 ± 0.06
90-78 x-ray TI image				
X-ray P ₀ (TI) (μm)	69.4 ± 1.7	66.2 ± 1.0	52.8 ± 6.8	48.1 ± 0.5
X-ray P ₂ /P ₀ (TI) (%)	-10.6 ± 1.7	6.2 ± 0.8	-6.8 ± 1.4	-1.0 ± 2.1

implosion also increased as a function of level of Kr. See Table I for the measured performance metrics listed. A subsequent publication will explore in greater detail the effects of this Kr premix on burn in an integrated ICF implosion, and here we will instead focus on the spectral data.

In an indirect-drive platform, care has to be taken to isolate x-ray emission from the region of interest (in our case the capsule hot-spot), as the hohlraum itself serves as a very bright, long duration x-ray source. In the initial experiment using 0.01 at. % Kr in the DD gas fill, only time-integrated spectral data were acquired using NXS viewing the implosion from the north pole (00-00) through the upper laser entrance hole (LEH). The Kr He- α complex could be identified; however there was a strong contribution from the Au hohlraum plasma. Au (L-shell) lines dominated the spectra, and the high level of background accentuated the crystal artifacts producing artifacts in the spectra.

For the follow-on experiment using 0.02 at. % Kr, the DISC was utilized on the central channel of the NXS to time-gate the implosion and thus separate the hohlraum emission from the capsule emission. The NXS again viewed the implosion through the 00-00 line of sight. The raw data are shown in Fig. 4(b), compared to the simultaneously collected time-integrated data in Fig. 4(a). As can be seen, the hohlraum emission follows the laser pulse and disappears soon after the laser turns off. The Kr emission does not appear until 1 ns later,

after the capsule has converged, and the hot-spot forms at high temperature and density around peak compression. Here we are able to identify Kr $n = 3-1$ and $n = 2-1$ lines. The overall duration of the Kr emission of ~ 250 ps is consistent with the x-ray burnwidth measured from other diagnostics.

In the final experiment using 0.03 at. % Kr, the NXS was moved to an equatorial line-of-sight at (90, 315). A hole was cut out of the Au hohlraum wall and replaced with a high-density carbon window of 160 μm thickness to transmit the x-ray emission from the capsule at stagnation. The window did not have an Au coating. From this view, the acquired spectra were very clean, with prominent Kr lines, and no strong Au lines, even on the time-integrated, in contrast to the 00-00 view. This is likely due to the fact that for the period of time where the lasers are on, the capsule overfills the window, so Au emission from the far side of the hohlraum is blocked from reaching the detector. The capsule does not begin accelerating inward until the lasers turn off, where (as demonstrated by the second shot) the Au quickly cools and stops radiating. This demonstrates the viability of doing spectroscopy (even time-integrated) on the equatorial axis.

In summary, time-resolved krypton K-shell line emission has been observed in indirectly driven ICF implosions, and can serve as a useful diagnostic to probe regions of interest. We are developing expertise in x-ray spectroscopy with a near-term focus on measuring the electron temperature in Kr-doped,

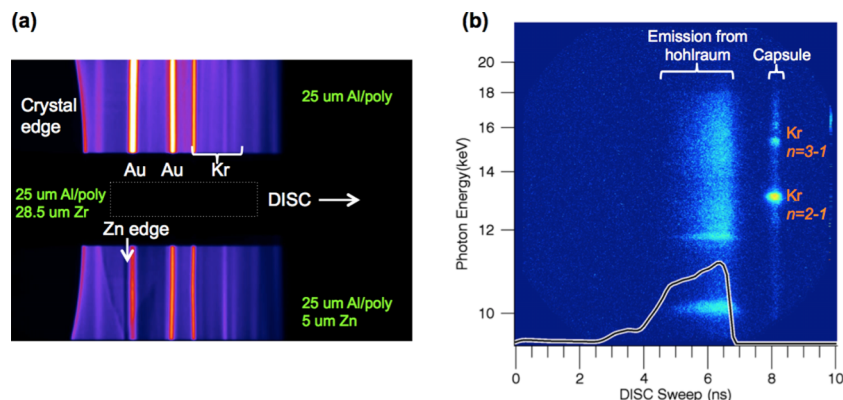


FIG. 4. (a) Time-integrated spectra recorded using NXS spectrometer viewing the implosion of a 0.02 at. % Kr-doped symcap through the north pole LEH. (b) The streaked spectra recorded from DISC on the same shot. The trace is the laser pulse. The time-resolved measurement eliminated the large background emission from the LEH and resulted in very clean Kr spectral data.

gas-filled symcaps. The principal goal has been met to demonstrate that the NXS spectrometer can measure Kr line spectra in this platform. The experimental measurements will be used to optimize the platform for future spectroscopic measurements of integrated ICF implosions on the NIF and to develop T_e extraction techniques.

The results of these shots are also being used to drive improvements to future platform fielding. This includes increasing the implosion temperature to optimize charge balance and enhance He- β emission, and improving the spectrometer to have higher spatial resolution. Better constraints on the models used in predictive simulations will require direct density and temperature measurements through line-ratio, Doppler-broadened, and Stark-broadened measurements of dopants in the hot-spot enabled by high-resolution spectrometers.

ACKNOWLEDGMENTS

We wish to thank the NIF operations team, in particular D. Holunga, T. Kohut, M. Chiarappa-Zucca, P. Amick, R. Mccracken, P. Epperson, and D. Trummer for their expertise and assistance in fielding and characterizing the krypton-doped gas capsules. This work was performed under the auspices of the U.S. Department of Energy by Lawrence Livermore National Laboratory under Contract No. DE-AC52-07NA27344.

¹J. D. Lindl, P. Amendt, R. L. Berger, S. G. Glendinning, S. H. Glenzer, S. W. Haan, R. L. Kauffman, O. L. Landen, and L. J. Suter, *Phys. Plasmas* **11**, 339 (2004).

- ²G. H. Miller, E. I. Moses, and C. R. Wuest, *Nucl. Fusion* **44**, S228 (2004).
- ³E. I. Moses, R. N. Boyd, B. A. Remington, C. J. Keane, and R. Al-Ayat, *Phys. Plasmas* **16**, 041006 (2009).
- ⁴M. Gatu Johnson *et al.*, "Indications of flow near maximum compression in layered deuterium-tritium capsule implosions at the National Ignition Facility," *Phys. Rev. E* (to be published).
- ⁵G. A. Kyrala *et al.*, *Phys. Plasmas* **18**, 056307 (2011).
- ⁶C. J. Keane, B. A. Hammel, D. R. Kania, J. D. Kilkenny, R. W. Lee, A. L. Osterheld, L. J. Suter, R. C. Mancini, C. F. Hooper, Jr., and N. D. Delamater, *Phys. Fluids B* **5**, 3328 (1993).
- ⁷B. A. Hammel, C. J. Keane, M. D. Cable, D. R. Kania, J. D. Kilkenny, R. W. Lee, and R. Pasha, *Phys. Rev. Lett.* **70**, 1263 (1993).
- ⁸S. P. Regan *et al.*, *Phys. Plasmas* **9**, 1357 (2002).
- ⁹N. C. Woolsey *et al.*, *J. Quant. Spectrosc. Radiat. Transfer* **58**, 975 (1997).
- ¹⁰A. R. Miles *et al.*, *Phys. Plasmas* **19**, 072702 (2012).
- ¹¹D. C. Wilson *et al.*, *J. Phys.: Conf. Ser.* **112**, 022015 (2008).
- ¹²J. R. Rygg *et al.*, *Phys. Plasmas* **13**, 052702 (2006).
- ¹³H. A. Scott, *J. Quant. Spectrosc. Radiat. Transf.* **71**, 689 (2001).
- ¹⁴M. Marinak *et al.*, *Phys. Plasmas* **5**, 1125 (1998).
- ¹⁵H.-K. Chung, M. H. Chen, W. L. Morgan, Y. Ralchenko, and R. W. Lee, *High Energy Density Phys.* **1**, 3 (2005), <http://nlte.nist.gov/FLY/>.
- ¹⁶T. Ma *et al.*, *Phys. Rev. Lett.* **111**, 085004 (2013).
- ¹⁷S. Le Pape *et al.*, *Phys. Plasmas* **23**, 056311 (2016).
- ¹⁸D. Turnbull *et al.*, *Phys. Plasmas* **23**, 052710 (2016).
- ¹⁹F. Perez *et al.*, *Rev. Sci. Instrum.* **85**, 11E613 (2014).
- ²⁰J. R. Kimbrough *et al.*, *Rev. Sci. Instrum.* **72**, 748 (2001).
- ²¹D. H. Kalantar *et al.*, *Rev. Sci. Instrum.* **72**, 751 (2001).
- ²²S. Glenn *et al.*, *Rev. Sci. Instrum.* **81**, 10E539 (2010).
- ²³G. A. Kyrala *et al.*, *Rev. Sci. Instrum.* **81**, 10E316 (2010).
- ²⁴T. Ma *et al.*, *Rev. Sci. Instrum.* **83**, 10E115 (2012).
- ²⁵N. Izumi *et al.*, *Rev. Sci. Instrum.* **83**, 10E121 (2012).
- ²⁶S. F. Khan *et al.*, *Proc. SPIE* **8505**, 850505 (2012).
- ²⁷A. B. Zylstra *et al.*, *Rev. Sci. Instrum.* **83**, 10D901 (2012).
- ²⁸V. Yu *et al.*, *Rev. Sci. Instrum.* **81**, 10D325 (2010).
- ²⁹R. A. Lerche *et al.*, *Rev. Sci. Instrum.* **81**, 10E319 (2010).
- ³⁰H. Rinderknecht *et al.*, *Rev. Sci. Instrum.* **83**, 10D902 (2012).